



Article

Isolation and Functional Characterization of Two *CONSTANS*-like 16 (*MiCOL16*) Genes from Mango

Yuan Liu [†], Cong Luo [†], Yihang Guo, Rongzhen Liang, Haixia Yu, Shuquan Chen, Xiao Mo, Xiaozhou Yang and Xinhua He ^{*}

State Key Laboratory for Conservation and Utilization of Subtropical Agro-Bioresources, College of Agriculture, National Demonstration Center for Experimental Plant Science Education, Guangxi University, Nanning 530004, China; 18638785643@163.com (Y.L.); 22003luocong@gxu.edu.cn (C.L.); yihang1066@163.com (Y.G.); liangrz0207@163.com (R.L.); yuhaixia0201@163.com (H.Y.); shuquanchen2022@163.com (S.C.); 18376683951@163.com (X.M.); yxz05206018@163.com (X.Y.)

* Correspondence: hexh@gxu.edu.cn

[†] These authors contributed equally to this work.

Abstract: *CONSTANS* (*CO*) is an important regulator of photoperiodic flowering and functions at a key position in the flowering regulatory network. Here, two *CO* homologs, *MiCOL16A* and *MiCOL16B*, were isolated from “SiJiMi” mango to elucidate the mechanisms controlling mango flowering. The *MiCOL16A* and *MiCOL16B* genes were highly expressed in the leaves and expressed at low levels in the buds and flowers. The expression levels of *MiCOL16A* and *MiCOL16B* increased during the flowering induction period but decreased during the flower organ development and flowering periods. The *MiCOL16A* gene was expressed in accordance with the circadian rhythm, and *MiCOL16B* expression was affected by diurnal variation, albeit not regularly. Both the *MiCOL16A* and *MiCOL16B* proteins were localized in the nucleus of cells and exerted transcriptional activity through their MR domains in yeast. Overexpression of both the *MiCOL16A* and *MiCOL16B* genes significantly repressed flowering in *Arabidopsis* under short-day (SD) and long-day (LD) conditions because they repressed the expression of *AtFT* and *AtSOC1*. This research also revealed that overexpression of *MiCOL16A* and *MiCOL16B* improved the salt and drought tolerance of *Arabidopsis*, conferring longer roots and higher survival rates to overexpression lines under drought and salt stress. Together, our results demonstrated that *MiCOL16A* and *MiCOL16B* not only regulate flowering but also play a role in the abiotic stress response in mango.

Keywords: mango; *CONSTANS*; flowering; functional analysis; abiotic stress



Citation: Liu, Y.; Luo, C.; Guo, Y.; Liang, R.; Yu, H.; Chen, S.; Mo, X.; Yang, X.; He, X. Isolation and Functional Characterization of Two *CONSTANS*-like 16 (*MiCOL16*) Genes from Mango. *Int. J. Mol. Sci.* **2022**, *23*, 3075. <https://doi.org/10.3390/ijms23063075>

Academic Editor: Zsófia Bánfalvi

Received: 12 February 2022

Accepted: 11 March 2022

Published: 12 March 2022

Publisher's Note: MDPI stays neutral with regard to jurisdictional claims in published maps and institutional affiliations.



Copyright: © 2022 by the authors. Licensee MDPI, Basel, Switzerland. This article is an open access article distributed under the terms and conditions of the Creative Commons Attribution (CC BY) license (<https://creativecommons.org/licenses/by/4.0/>).

1. Introduction

In higher plants, floral transition is the process that describes the switch from the vegetative stage to the reproductive stage. The time for this process is referred to as flowering time. The flowering mechanism of the annual plant species *Arabidopsis* is thoroughly understood. According to recent research, the onset of flowering is regulated in a timely manner by an intricate network involving a series of regulatory pathways, such as gibberellin, photoperiod, autonomous, aging and vernalization pathways [1–3]. Of the many regulatory pathways, the photoperiod pathway is especially important; it is involved in plant responses to photoperiod sensing and subsequent molecular events [4].

Many photoperiod pathway-related genes have been discovered, such as TIME OF CAB EXPRESSION 1 (TOC1), LATE ELONGATED HYPOCOTYL (LHY), EARLY FLOWERING 4 (ELF4), GIGANTEA (GI), CIRCADIAN CLOCK ASSOCIATED 1 (CCA1), FLOWERING LOCUS T (FT) and *CONSTANS* (*CO*) [5]. Among them, *CO* is a key component of which there are orthologs in various plant species [6–9]. Currently, CYCLING DOF FACTOR (CDF) is known as the only transcription factor that directly binds to the *CO* promoter and suppresses the expression of *CO* [10–12]. The *GI* gene plays a key role in the

photoperiod induction pathway and positively regulates the expression of the CO gene under long-day conditions [13]. Overexpression of the FLOWERING BHLH (FBH) gene elevates CO levels without being affected by photoperiod [14]. In addition, phytochrome-interacting factors (PIFs) interact with CO to suppress flowering [15]. The E3 ubiquitin ligase-encoding gene HIGH EXPRESSION OF OSMOTICALLY RESPONSIVE GENES1 (HOS1) is involved in controlling the abundance of CO, and CONSTITUTIVE PHOTOMORPHOGENIC1 (COP1), as a flowering repressor, is regulated by cryptochromes (CRY) and promotes the proteolysis of CO in the dark [16,17]. CO genes belong to the BBX family and can be divided into three categories according to their domains in Arabidopsis [7,18]. Group I genes have one CO, CO-like, and TOC1 (CCT) domain and two B-box domains; group II genes have one B-box and one CCT domain; and group III genes have one B-box, one variant B-box and one CCT domain.

However, the functions of CO orthologs vary across different species. In *Arabidopsis*, overexpression of the *AtCO*, *AtCOL5* and *AtCOL16* genes promotes flowering under long-day (LD) or short-day (SD) conditions [19,20], but *AtCOL7*, *AtCOL8* and *AtCOL9* inhibit flowering under LD conditions [21,22]. In rice, the *OsHd1* gene delays flowering under LD conditions and promotes flowering under SD conditions [23], and *OsCOL16* inhibits flowering under both SD and LD conditions [24]. *StCO*, a CO homolog in potato, regulates flowering [25]. Moreover, the CO orthologs in Fuji apple, *MdCOL1* and *MdCOL2*, play a significant role in the growth and development of reproductive organs [26]. Thus, homologous CO genes have a wide range of effects on plant flowering and development.

Mango (*Mangifera indica* L.) is a member of the Anacardiaceae family and is an economically important fruit tree species. Flowering time has a considerable influence on the yield and quality of mango. Therefore, the discovery and identification of flowering-related genes are necessary for mango production. Mango flowering is the result of a complex process influenced by many factors, but it is not affected by daylength [27]. Several flowering-related regulatory genes have recently been identified in mango. For example, the *MiFT*, *MiSOC1* and *MiAP1* genes promote flowering, but the *MiCO* gene inhibits flowering in *Arabidopsis* [28–31]. However, the *COL16* gene has not been studied in mango. Here, we isolated two COL genes, *MiCOL16A* and *MiCOL16B*, and verified their function. Our results indicated that these two genes strongly influence the flowering and abiotic stress responses of mango.

2. Results

2.1. Isolation and Analysis of *MiCOL16A* and *MiCOL16B*

Two CO homologs, *MiCOL16A* (GenBank No: MW326761) and *MiCOL16B* (GenBank No: MW326762), were identified from *M. indica* L. cv. SiJiMi. The full cDNA sequences of *MiCOL16A* and *MiCOL16B* were 1269 bp and 1251 bp, encoding 423 and 417 amino acids, respectively; the two genes were 73.06% identical. The DNA sequences of *MiCOL16A* and *MiCOL16B* were 2030 bp and 1751 bp, respectively, and each contained one intron (Figure 1A). The alignment of *MiCOL16A* and *MiCOL16B* indicated that both have one CCT and one B-box domain and are highly conserved with other genes (Figure 1B). Phylogenetic analysis showed that these two genes were highly identical to *Arabidopsis AtCOL6* and *AtCOL16* in group II (Figure 1C). Therefore, these results indicated that *MiCOL16A* and *MiCOL16B* belong to group II genes of the CO gene family.

2.2. Expression of *MiCOL16A* and *MiCOL16B* in Mango

For the tissue-specific expression tests, qRT-PCR was performed. The results showed that *MiCOL16A* and *MiCOL16B* were expressed in all the tested tissues. On different branches, the expression levels of *MiCOL16A* and *MiCOL16B* in the leaves were always higher than those in the stems, buds or flowers, and the lowest expression levels of *MiCOL16A* and *MiCOL16B* were detected in the buds and flowers. In contrast, the expression level of *MiCOL16A* in the leaves of nonflowering branches was higher than that in the

leaves of flowering branches (Figure 2A), but *MiCOL16B* expression was lower in the leaves of nonflowering branches than in those of flowering branches (Figure 2B).

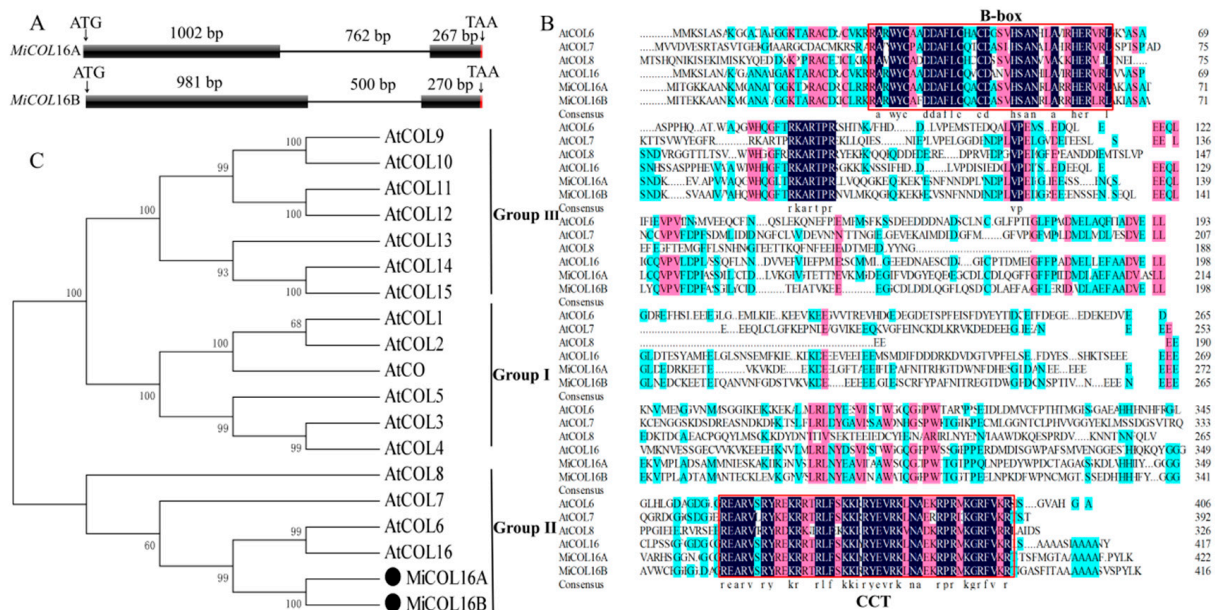


Figure 1. Sequence analysis of *MiCOL16A* and *MiCOL16B*. (A) Genomic structures of *MiCOL16A* and *MiCOL16B*. Exons are represented by black squares, and introns are represented by black lines. The numbers indicate the lengths of the corresponding regions. (B) Alignment of the predicted amino acid sequences of AtCOL6–8 and AtCOL16 in *Arabidopsis* and of *MiCOL16A* and *MiCOL16B* in mango. The conserved CCT and B-box domain regions are indicated with red boxes. The dark color indicates that the amino acids are 100% conserved. The genes and their accession numbers are shown in Supplementary Table S1. (C) Phylogenetic relationship of CO/COL proteins in *Arabidopsis* and mango. *MiCOL16A* and *MiCOL16B* are represented by black solid circles.

To analyze the temporal expression patterns of *MiCOL16A* and *MiCOL16B*, qRT-PCR was performed. The results suggested that the two target genes were expressed in the leaves of mango at all tested periods. The expression pattern of *MiCOL16A* gradually increased from vegetative growth to the late floral induction period and then decreased (Figure 2C). However, *MiCOL16B* gene expression increased during the vegetative growth period to the early floral induction period and then decreased (Figure 2D).

The circadian-driven expression of *MiCOL16A* and *MiCOL16B* was determined using total RNA isolated from ‘SiJiMi’ mango leaves, which were collected every 3 h for three days. The results suggested that under LD conditions, the expression level of *MiCOL16A* started to increase after dusk, peaked 6 h after dusk and decreased rapidly thereafter before beginning to increase again after dusk (Figure 3A). Interestingly, this pattern also appeared under MD and SD conditions, and this result proved that *MiCOL16A* expression may be induced by night treatment and is not affected by the length of light (Figure 3C,E). The expression level of *MiCOL16B* fluctuated with time under different conditions, but there was no regularity. These results suggest that *MiCOL16A* expression exhibits a diurnal oscillation rhythm, but *MiCOL16B* expression is not affected by a diurnal rhythm (Figure 3B,D,F).

2.3. Both *MiCOL16A* and *MiCOL16B* Are Nuclear Proteins with Transcriptional Activation Activity

MiCOL16A and *MiCOL16B* protein-linked GFP fusion constructs driven by the CaMV 35S promoter were developed for molecular function assays. The GFP fusion constructs were inserted into vectors, which were transferred into onion inner epidermal cells. Single-strand analysis indicated that free GFP localized to the nucleus and cytomembrane, and both the *MiCOL16A* and *MiCOL16B* proteins localized to the nucleus (Figure 4A).

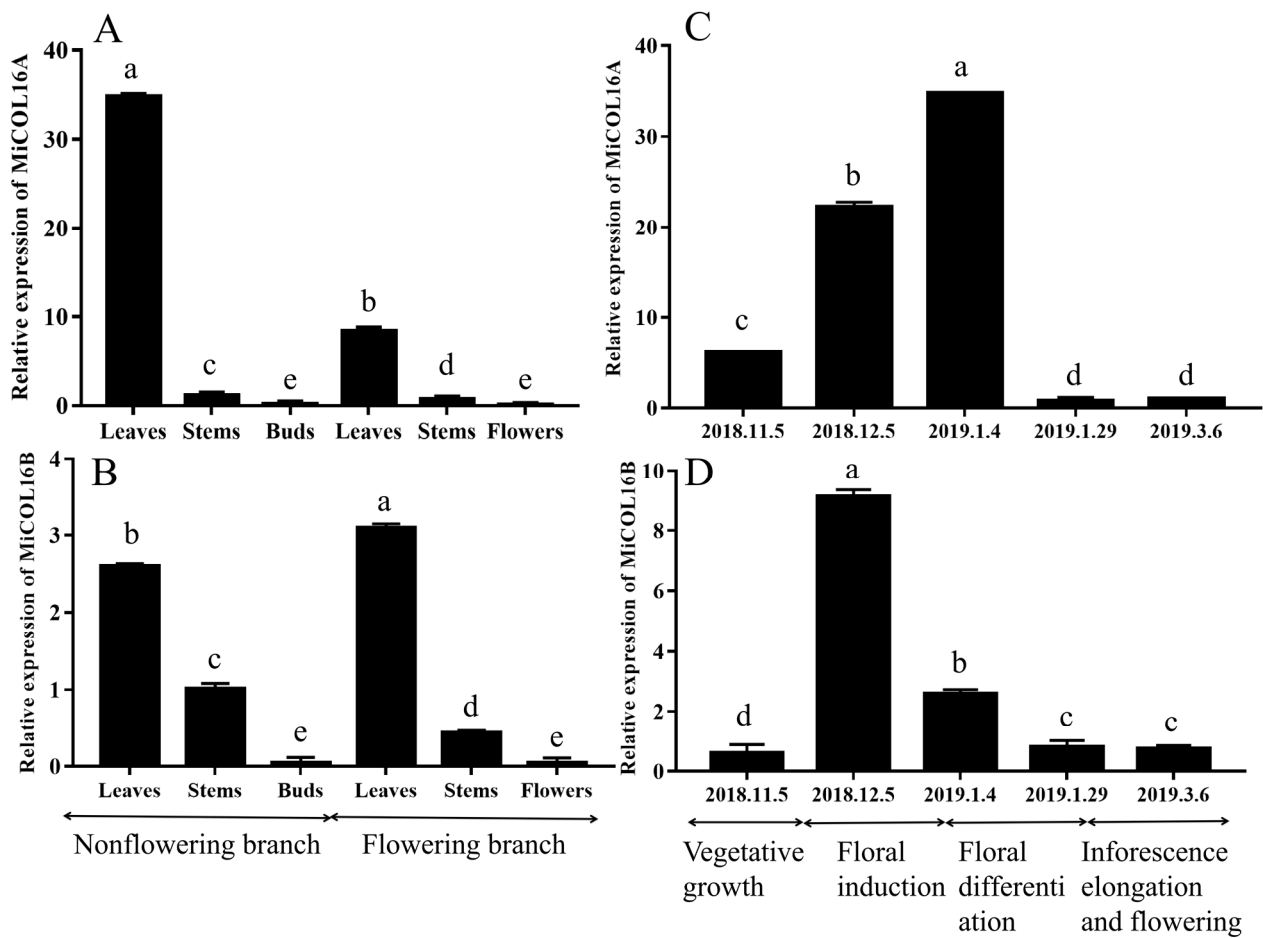


Figure 2. Tissue-specific and temporal expression analysis of the *MiCOL16A* and *MiCOL16B* genes. (A,B) Expression patterns of the *MiCOL16A* and *MiCOL16B* genes in different tissues of SiJiMi mango. (C,D) Expression patterns of the *MiCOL16A* and *MiCOL16B* genes at different time points.

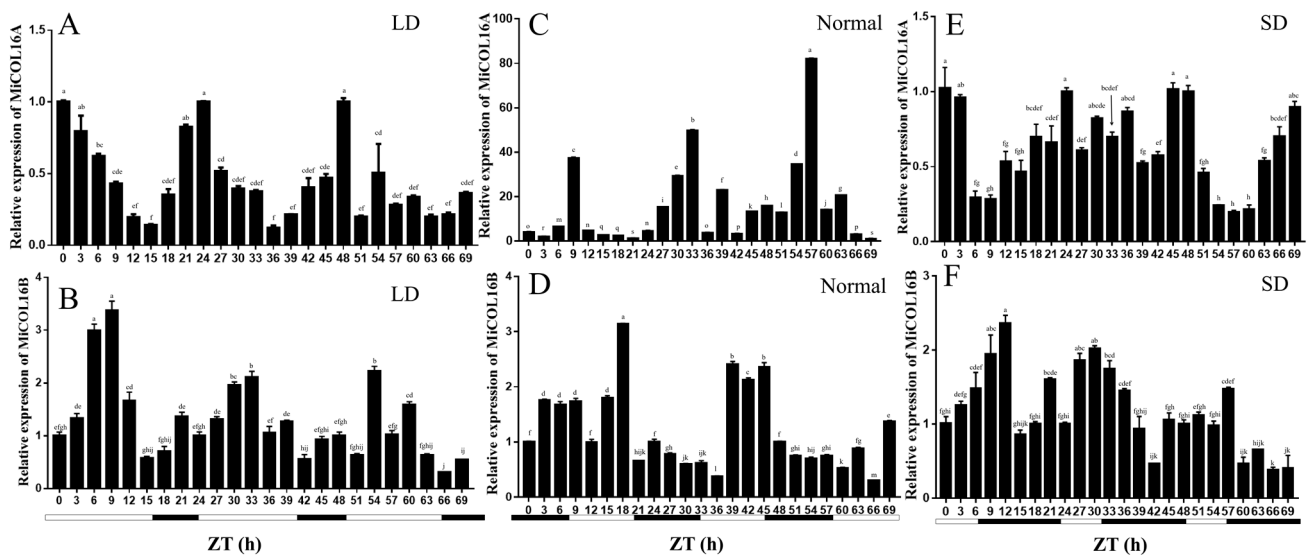


Figure 3. Expression analysis of the *MiCOL16A* and *MiCOL16B* genes in terms of circadian rhythm. (A,C,E) Expression patterns of *MiCOL16A* under LD (A), normal (C) and SD (E) conditions. (B,D,F) Expression patterns of *MiCOL16B* under LD (B), normal (D) and SD (F) conditions.

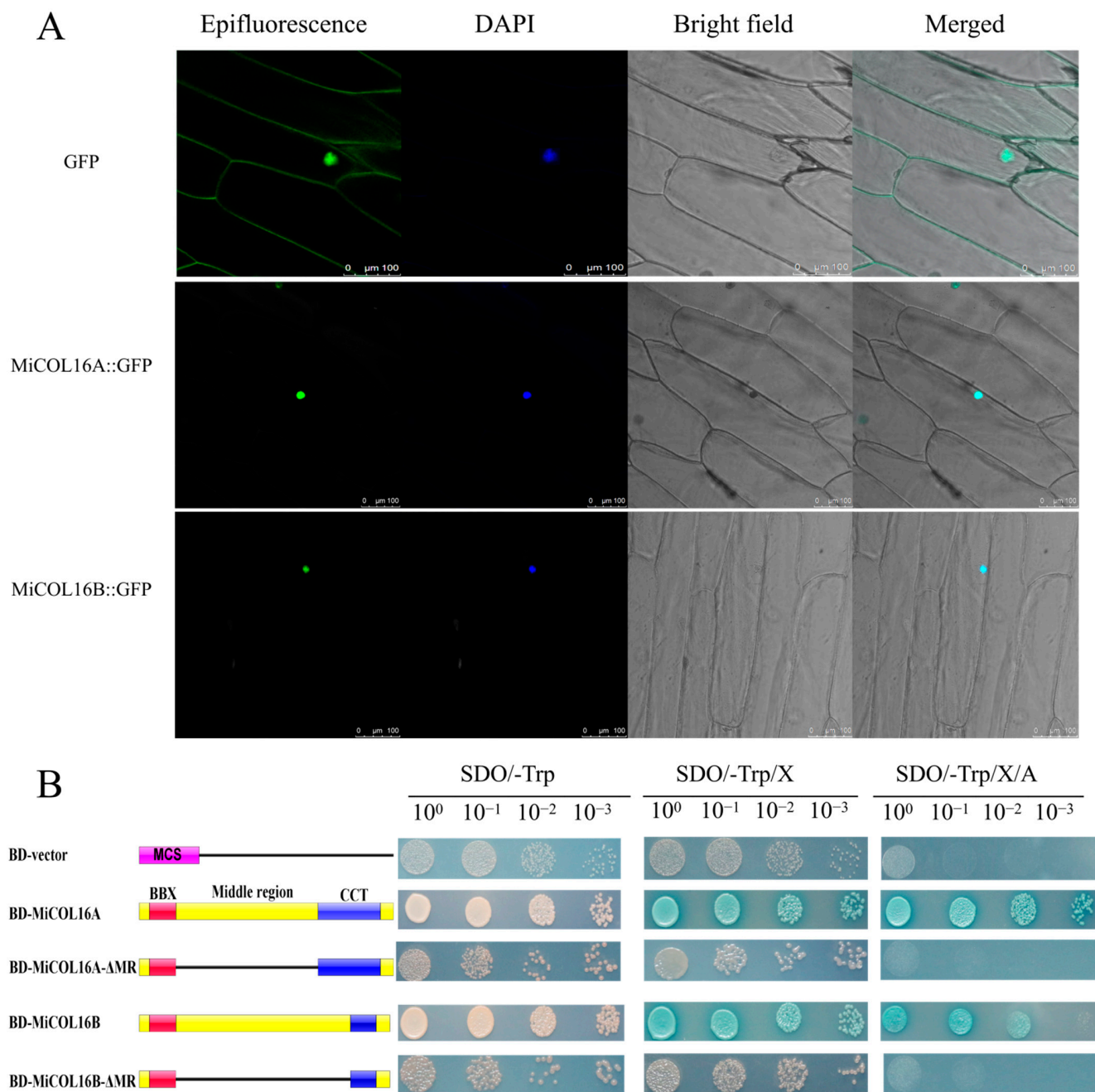


Figure 4. (A) Subcellular localization. Scale bars = 100 μ m. (B) Transcriptional activation activity. The left diagram shows various constructs. MCS, multiple cloning sites; BD, GAL4-DNA binding domain; BBX, B-box; CCT, CO, CO-like, TOC1; MR, middle region.

A transcriptional activity assay was performed in yeast cells to demonstrate whether *MiCOL16A* or *MiCOL16B* had transcriptional activation activity. According to a previous study, the MR between the B-BOX and CCT domains is required for CO transcriptional activity [24,32,33]. Thus, *MiCOL16A*, *MiCOL16B*, *MiCOL16A*- Δ MR and *MiCOL16B*- Δ MR were fused into a pGBKT7 vector, and an empty pGBKT7 vector was used as a control. The five different plasmids were transferred into yeast cells, which were then transferred onto different plates. Three days later, all the transformants grew equally well on selective SD/-Trp media. On these three selective media, the BD-MiCOL16A and BD-MiCOL16B transformants grew well and turned blue, but the yeast transformed with the BD-vector, BD-MiCOL16A- Δ MR and BD-MiCOL16B- Δ MR grew only on SD/-Trp/X- α -gal plates and did not turn blue (Figure 4B). Together, α -gal activity could not be detected when the MR

region was deleted. These results showed that through their MR domains, *MiCOL16A* and *MiCOL16B* have transcriptional activation activity in yeast.

2.4. Overexpression of *MiCOL16A* and *MiCOL16B* Delayed Flowering in *Arabidopsis*

To determine whether *MiCOL16A* and *MiCOL16B* are involved in the regulation of flowering time, they were overexpressed in *Arabidopsis* (under the control of the CaMV 35S promoter). We obtained 15 and 10 independent transgenic lines of *MiCOL16A* and *MiCOL16B*, respectively, and we selected three homozygous lines for each construct from within the T3 generation and planted them under LD or SD conditions. The PCR analysis results showed that *MiCOL16A* and *MiCOL16B* were expressed in the transgenic plants but not in the WT or empty vector-transformed *Arabidopsis* plants under LD (Figure 5(A1,B1)) or SD conditions (Figure 6(A1,B1)). Under LD and SD conditions, both the *MiCOL16A* and *MiCOL16B* transgenic lines flowered later than the WT and empty vector-transformed plants. At flowering, compared with the WT and empty vector-transformed plants, the *MiCOL16A* and *MiCOL16B* transgenic plants had more rosette leaves (Figures 5 and 6) (Table 1).

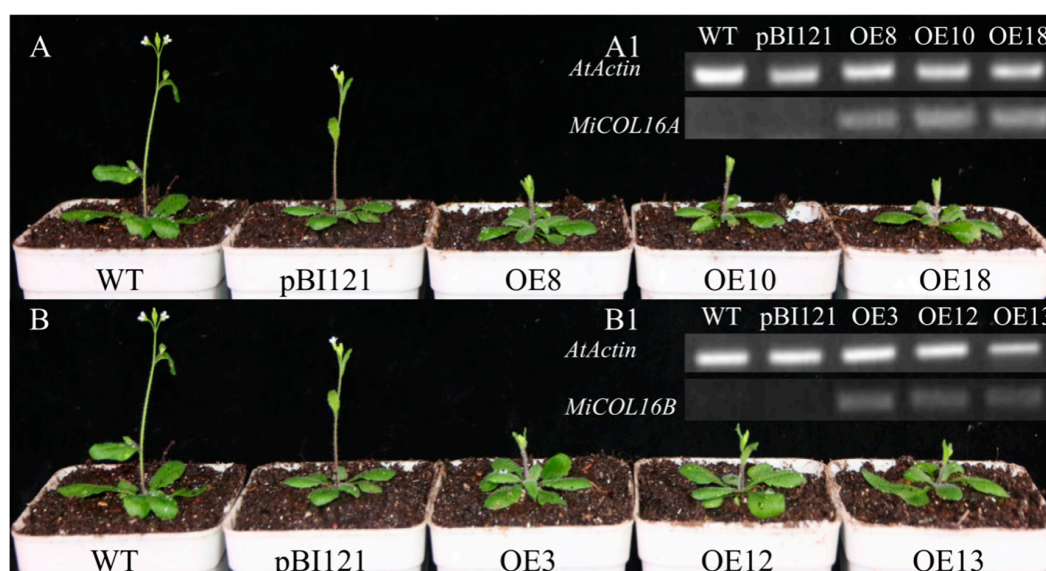


Figure 5. Ectopic expression of *MiCOL16A* and *MiCOL16B* delayed flowering under LD conditions. (A1,B1) Expression of *MiCOL16A* (A1) and *MiCOL16B* (B1) in the WT, empty vector-transformed and overexpression plants. (A) *MiCOL16A* transgenic *Arabidopsis* plants under LD conditions. (B) *MiCOL16B* transgenic *Arabidopsis* plants under LD conditions.

Table 1. Overexpression of *MiCOL16A* and *MiCOL16B* repressed flowering in *Arabidopsis*.

ID	Days to Flowering		No. Rosette Leaves		Plant Height ^a (cm)	
	LD	SD	LD	SD	LD	SD
WT	24.8 ± 0.6	50.1 ± 0.8	5.5 ± 0.5	7.2 ± 0.3	6.4 ± 0.8	11.4 ± 0.6
pBI121	25.6 ± 0.4	49.6 ± 0.7	7.6 ± 0.6	7.0 ± 0.5	6.7 ± 0.4	11.7 ± 0.4
<i>MiCOL16A</i>						
OE2	28.0 ± 0.3 *	51.3 ± 0.8	6.3 ± 0.4	7.6 ± 0.3	4.6 ± 1.1 *	14.2 ± 0.9 *
OE8	28.0 ± 0.5 *	52.8 ± 0.2 *	6.8 ± 0.6 *	7.3 ± 0.7	4.5 ± 0.6 *	14.2 ± 0.8 *
OE10	28.1 ± 0.8 *	52.8 ± 0.3 *	7.5 ± 1.0 *	7.3 ± 0.5	6.2 ± 1.1	13.0 ± 0.3 *
<i>MiCOL16B</i>						
OE3	27.6 ± 0.5 *	53.0 ± 0.4 *	6.6 ± 0.7 *	7.4 ± 0.6	4.7 ± 1.0 *	17.7 ± 1.1 *
OE12	26.9 ± 0.8 *	51.2 ± 0.9	7.1 ± 0.5 *	7.3 ± 0.4	5.2 ± 1.1 *	17.1 ± 1.0 *
OE13	28.4 ± 0.5 *	51.5 ± 0.4 *	6.7 ± 0.7 *	6.6 ± 0.6	4.3 ± 0.8 *	13.4 ± 0.2 *

^a Plant height was measured at the time of flowering. Significant differences among the samples were assessed at the $p < 0.05$ (*) level by Student's *t* tests.

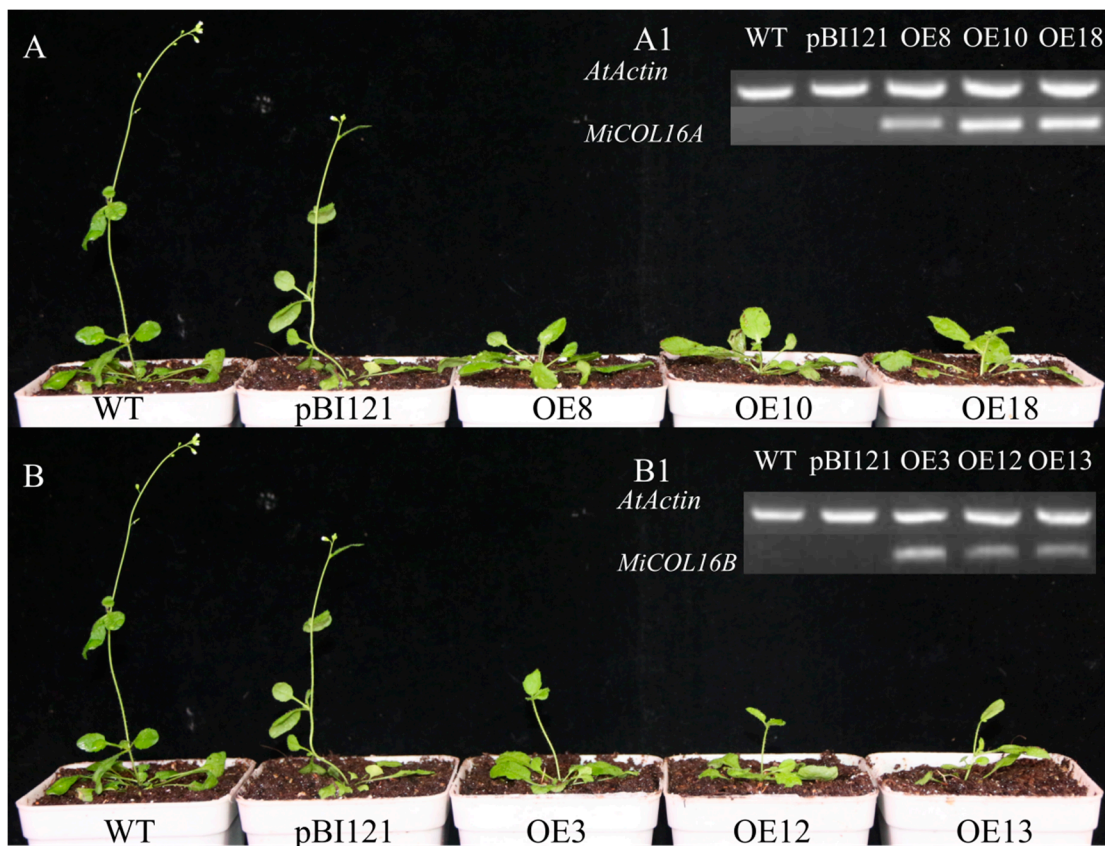


Figure 6. Ectopic expression of *MiCOL16A* and *MiCOL16B* delayed flowering under SD conditions. (A1,B1) Expression of *MiCOL16A* (A1) and *MiCOL16B* (B1) in the WT, empty vector-transformed and overexpression plants. (A) *MiCOL16A* transgenic *Arabidopsis* plants under SD conditions. (B) *MiCOL16B* transgenic *Arabidopsis* plants under SD conditions.

To further dissect the expression patterns of the floral integrator genes in the *MiCOL16A* and *MiCOL16B* overexpression lines, the transcript levels of *AtFT* and *AtSOC1* were measured in the WT and overexpression plants under LD or SD conditions (Figure 7). The results showed that both *MiCOL16A* and *MiCOL16B* significantly repressed the expression of *AtSOC1* and *AtFT* in *Arabidopsis* under LD and SD conditions.

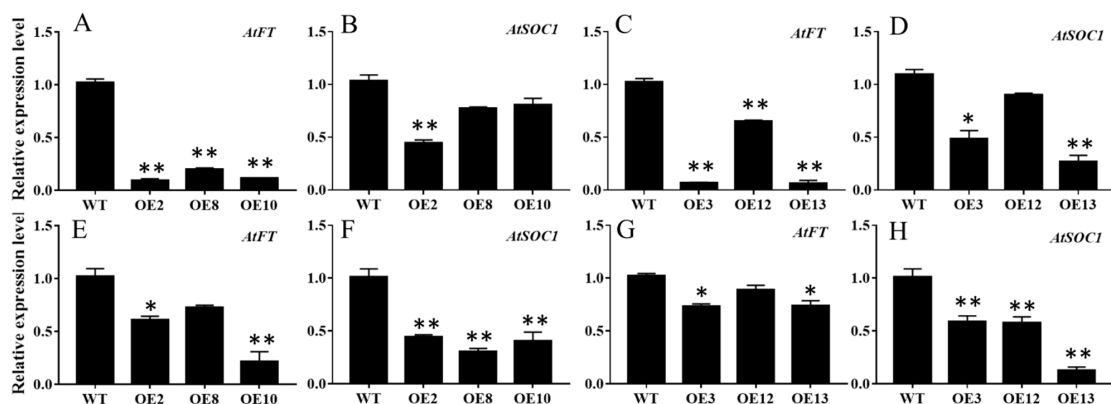


Figure 7. Expression patterns of flowering-related genes. (A–D) Expression patterns of *AtFT* and *AtSOC1* in the WT and the *MiCOL16A* (A,B) or *MiCOL16B* (C,D) overexpression plants under LD conditions. (E–H) Expression levels of *AtFT* and *AtSOC1* in the WT and the *MiCOL16A* (E,F) or *MiCOL16B* (G,H) overexpression plants under SD conditions. Significant differences among the samples were assessed at the $p < 0.05$ (*) and $p < 0.01$ (**) levels by Student’s *t* tests.

2.5. *MiCOL16A* and *MiCOL16B* Enhance Tolerance to Abiotic Stress

To assess the effect of ectopic *MiCOL16A* and *MiCOL16B* expression in response to abiotic stress, three homozygous lines (T3 generation) were selected. Three-day-old seedlings of the overexpression and WT plants were transplanted onto half-strength MS media supplemented with mannitol and NaCl. The length of their roots was measured after 7 days of stress treatment. The untreated WT and overexpression plants did not significantly differ, but compared with the WT plants, both *MiCOL16A* and *MiCOL16B* overexpression plants grew better and had longer roots under all stress conditions (Figures 8 and 9). Together, these results showed that, compared with WT plants, *MiCOL16A* and *MiCOL16B* transgenic plants had improved tolerance to drought and salt stress.

To further determine the response of *MiCOL16A* and *MiCOL16B* transgenic plants to abiotic stress, 7-day-old seedlings were transplanted into square pots. After the seedlings were allowed to recover, they were watered with 300 mM NaCl every 2 days, and regular water was withheld (Figure 10A,B). For salt treatment, the survival rate was measured when obvious phenotypic differences occurred. Approximately 20.0% of WT plants, 80.0% of *OEMiCOL16A*#3 plants, 93.3% of *OEMiCOL16A*#6 plants and 86.7% of *OEMiCOL16A*#10 plants survived (Figure 10C). Similarly, approximately 26.7% of WT plants survived, but 73.3% of *OEMiCOL16B*#3, 93.3% of *OEMiCOL16B*#12 and 86.7% of *OEMiCOL16B*#13 plants survived (Figure 10D). With respect to the drought treatment, the survival rate was measured after the plants had been rewatered for 3 days: a total of 6.7% of WT plants survived, but 93.3% of *OEMiCOL16A*#3, 80.0% of *OEMiCOL16A*#6 and 73.3% of *OEMiCOL16A*#10 plants survived (Figure 10C). Similarly, no WT survived, but 40.0% of *OEMiCOL16B*#3, 93.3% of *OEMiCOL16B*#12 and 80.0% of *OEMiCOL16B*#13 lines survived (Figure 10D). Together, these results showed that overexpression of *MiCOL16A* and *MiCOL16B* in *Arabidopsis* improved salt and drought tolerance.

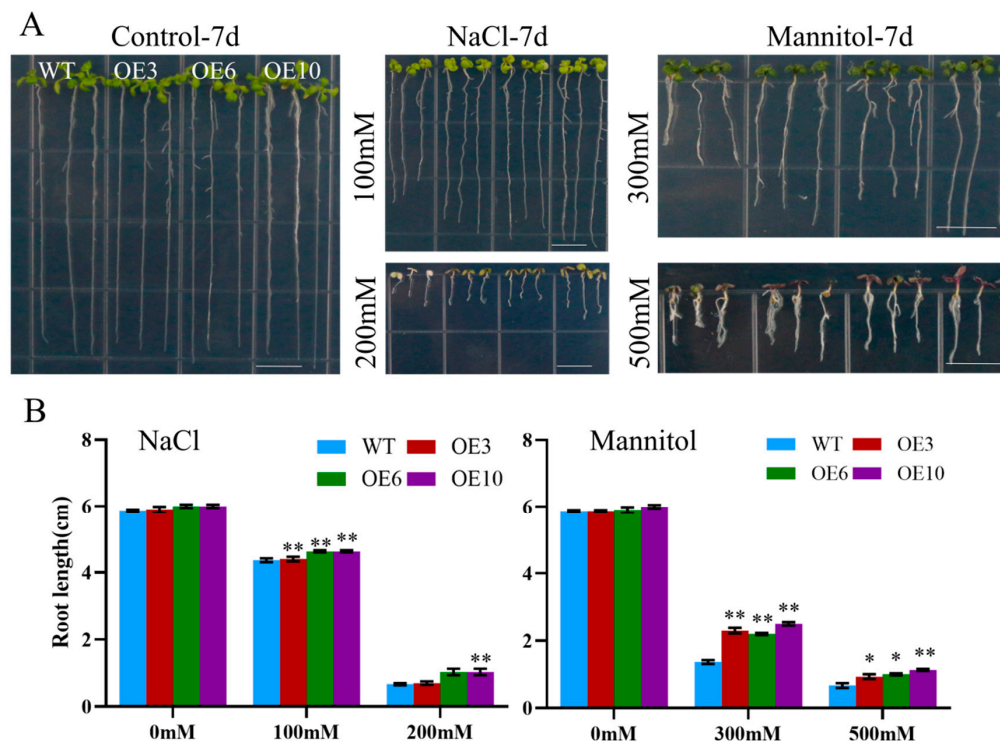


Figure 8. Assays of the length of the primary roots of WT and *MiCOL16A* transgenic lines under abiotic stress. (A) Seeds of the WT and three transgenic lines grown on half-strength MS media and subjected to various stresses. The bars represent 1.0 cm. (B) Lengths of the roots of all the lines under salt and drought treatment. Significant differences among the samples were assessed at the $p < 0.05$ (*) and $p < 0.01$ (**) levels by Student's *t* tests.

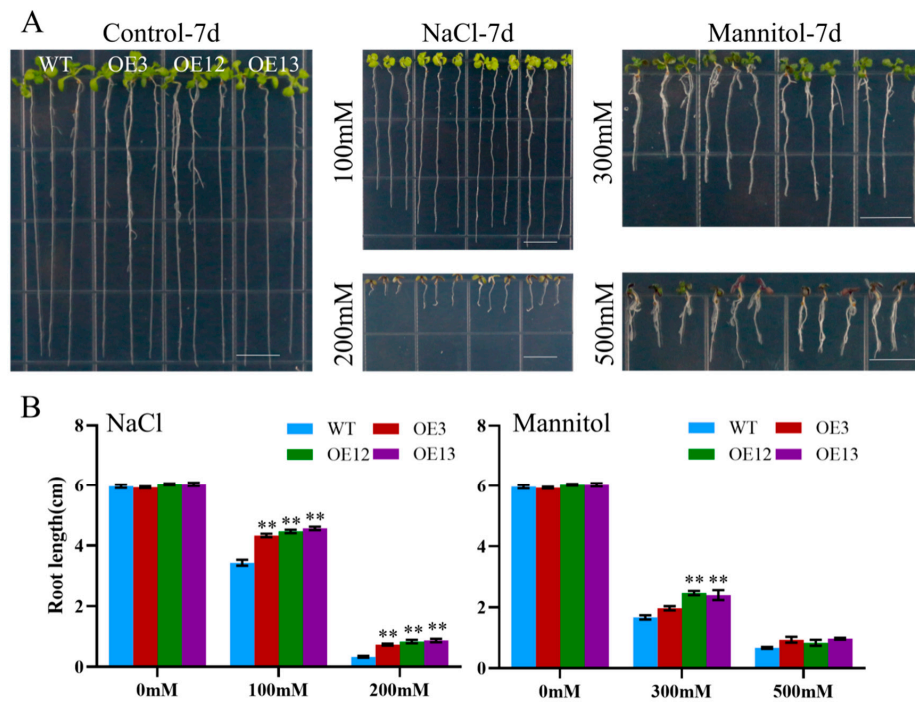


Figure 9. Assays of the length of the primary roots of the WT and *MiCOL16B* transgenic lines under abiotic stress. (A) Seeds of the WT and three transgenic lines grown on half-strength MS media and subjected to various stresses. The bars represent 1.0 cm. (B) Lengths of the roots of all the lines under salt and drought treatment. Significant differences among the samples were assessed at the $p < 0.01$ (**) levels by Student's *t* tests.

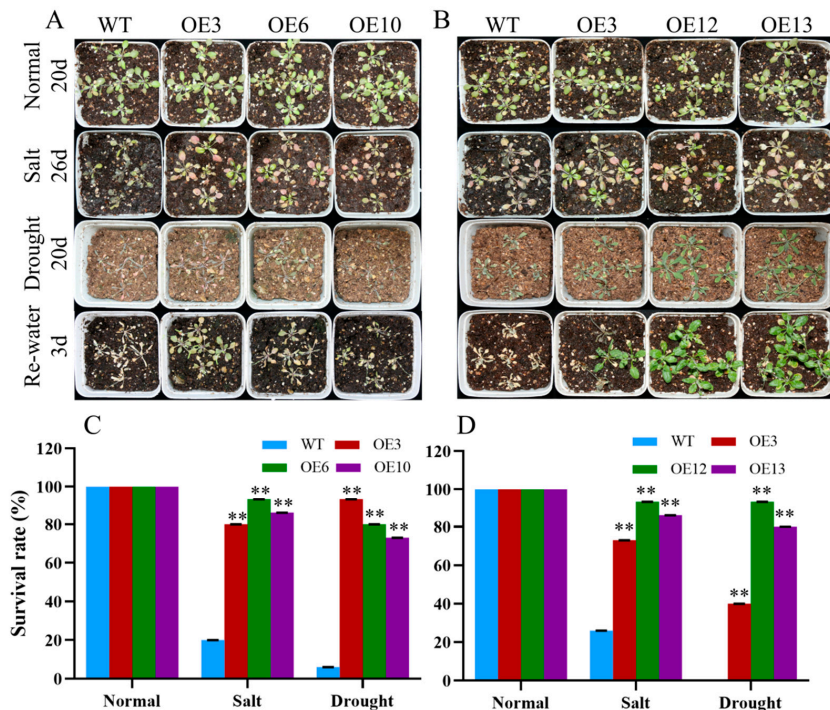


Figure 10. Phenotypes of WT and *MiCOL16A* and *MiCOL16B* transgenic plants under abiotic stresses. Normal, control; salt, 300 mM NaCl solution applied every 2 days; drought, withholding of water. (A) WT and *MiCOL16A* transgenic plants under different stresses. (B) WT and *MiCOL16B* transgenic lines under different stresses. (C–D) Survival rates of the WT and the *MiCOL16A* (C) and *MiCOL16B* (D) transgenic lines under different stresses. Significant differences among the samples were assessed at the $p < 0.01$ (**) levels by Student's *t* tests.

To explore the molecular mechanism underlying these phenomena in the transgenic lines in response to salt or drought, four stress-related genes were selected: *AtNHX1*, *AtRD20*, *AtSOS1* and *AtCOR15A* (Figure 11). Under salt stress, the expression levels of *AtNHX1*, *AtRD20* and *AtSOS1* were significantly higher in the three transgenic lines of *MiCOL16A* than in the WT, but in the *MiCOL16B* transgenic lines, the expression level of *AtRD20* was not significantly higher (Figure 11A,B). Under drought conditions, the expression levels of *AtCOR15A*, *AtRD20* and *AtNHX1* in the *MiCOL16A* and *MiCOL16B* transgenic lines were significantly higher than those in the WT (Figure 11C,D). These findings showed that by regulating the expression of stress-responsive genes, the *MiCOL16A* and *MiCOL16B* genes might increase the stress tolerance of transgenic plants under drought or salt stress.

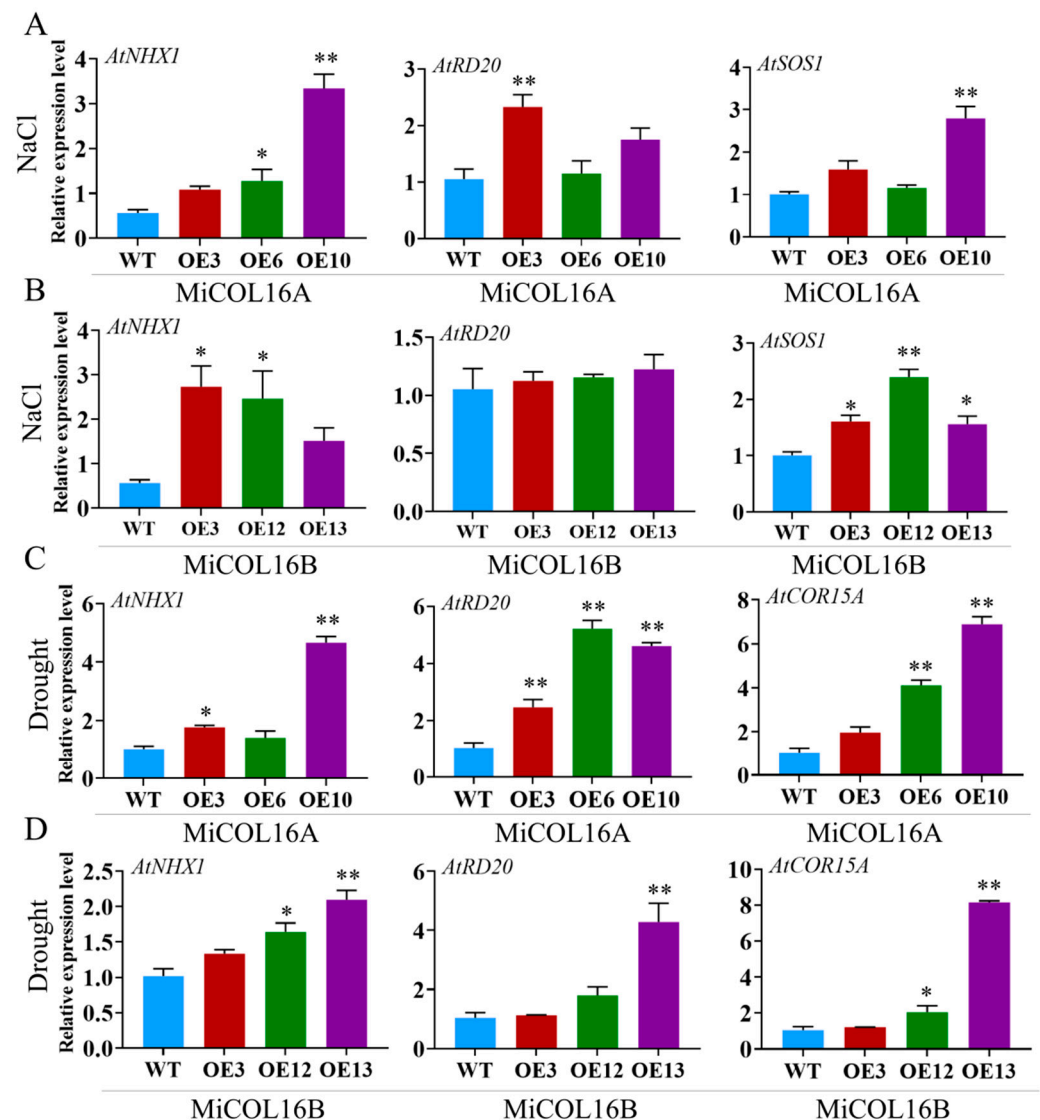


Figure 11. Expression patterns of stress-responsive genes in WT and *MiCOL16A* and *MiCOL16B* transgenic lines. (A,B) Salt stress conditions. Expression levels of the *AtNHX1*, *AtRD20* and *AtSOS1* genes in *MiCOL16A* (A) and *MiCOL16B* (B) transgenic lines. (C,D) Drought stress conditions. Expression levels of the *AtNHX1*, *AtRD20* and *AtCOR15A* genes in the *MiCOL16A* (C) and *MiCOL16B* (D) transgenic lines. Significant differences among the samples were assessed at the $p < 0.05$ (*) and $p < 0.01$ (**) levels by Student's t tests.

3. Discussion

Flowering is an important event in the life cycle of plants. Mango, a typical perennial and economically important fruit tree species, is distributed mainly in tropical and subtropical areas, and its economic benefits are greatly affected by flowering time. Therefore, successfully controlling flowering time is critically important in mango production. The *CO* gene plays an indispensable role in the photoperiodic pathway and regulates the flowering time of plants [34]. In a previous study, more than 36 *CO* homologs were identified from mango transcriptomic data [27]. Here, we identified and characterized two zinc finger *COL16* protein orthologs, *MiCOL16A* and *MiCOL16B*, in mango. Bioinformatic analysis indicated that both *MiCOL16* proteins are highly homologous to *AtCOL16* and have only one CCT and one B-box domain, thus belonging to group II of the *CO* gene family.

CO/COL genes are the key genes controlling flowering in plants. These genes are regulated by the upstream gene *GI* [23,35] and control the downstream gene *FT*, thereby inducing flowering in plants [36]. Studies have shown that the leaves are the plant organs that initially perceive photoperiodic signals [37], and the synthesis of *FT* proteins controlled by the *CO* gene is also observed to occur in the leaves [38,39]. In this study, the expression patterns of the *MiCOL16A* and *MiCOL16B* genes in SiJiMi showed that both genes were highly expressed in the leaves, especially during the vegetative phase, but were expressed at low levels in the flowers (Figure 2). Similarly, the *GbCOL16* gene in *Ginkgo biloba* is most highly expressed in the leaves [40], and the *BvCOL1* gene in *Beta vulgaris* is most highly expressed in cauline leaves and less so in the buds and roots [41]. In petunia, *PhCOL16* homologs are involved in chlorophyll accumulation and have higher expression levels in leaves [42]. Moreover, *OsCOL16* in rice is expressed mainly in the youngest leaf blade, and the *VviCOL16a* genes in *Vitis vinifera* were expressed the most in the leaves [24,43]. In contrast, the highest expression level of *MiCOL16A* was found in the leaves of nonflowering branches and during the late floral induction period, but the *MiCOL16B* gene was expressed mainly in the leaves of flowering branches and during the early floral induction period.

In general, *CO* genes are affected by the circadian rhythm. In *Arabidopsis*, the expression level of *AtCO* peaks at dusk under LD conditions but peaks at night under SD conditions [44]. In *Cymbidium goeringii*, *CgCOL* is expressed at higher levels in the light than in the dark under LD conditions but at lower levels in the light than in the dark under SD conditions [45]. In *Chrysanthemum morifolium*, *CmCOL* expression peaks at 4:00 and 16:00 under both SD and LD conditions. Moreover, the expression level of the *OsCOL16* gene in rice increases after decreasing under both SD and LD conditions but peaks at 6 h or 14 h after dusk [24]. In the present study, the expression of *MiCOL16A* increased in the dark and decreased in the light. However, *MiCO* gene expression was greatest at 9:00 but then decreased under normal light conditions [31]. This result may be related to the structural differences of the genes. In the present study, the *MiCOL16A* gene was found to be involved in the circadian rhythm, but the *MiCOL16B* gene did not exhibit any regularity. The difference in the expression levels of these two genes may be caused by homologous differences.

According to the results, the *MiCOL16A* and *MiCOL16B* proteins localized to the nucleus of onion cells, and both have transcriptional activation activity through their MR domains. In rice, *OsCOL10*, *OsCOL15* and *OsCOL16* have one CCT and one B-box domain; they localize to the nucleus and display transcriptional activity through their MR domain [24,32,33]. Moreover, the protein encoded by *AtCOL7* in *Arabidopsis*, which has one B-BOX and one CCT domain, has been reported to be the key segment exhibiting transcriptional activity between the B-box and CCT domains [46]. The results in this report also confirmed the results of the present experiment.

CO acts at the center of the coordinate input mechanism that responds to light. The flowering time-controlling molecular mechanisms in *Arabidopsis* and rice have been studied extensively [47]. In *Arabidopsis*, the *CO* gene promotes flowering under LD conditions but inhibits flowering under SD conditions [8], and overexpression of the *COL16* gene can lead to slightly early flowering under LD conditions [20]. In addition, the *COL4* gene

represses flowering under LD or SD conditions [48]; the structure of both *COL7* and *COL8* is similar to that of *MiCOL16*, and these genes delay flowering under LD conditions [21,22]. In rice, *OsHd1* represses flowering only under LD conditions [8], *OsCO3* delays flowering time under SD conditions [49], and *OsCOL16* inhibits flowering under both SD and LD conditions [24]. In the present experiment, both *MiCOL16A* and *MiCOL16B* inhibited the flowering of the transgenic plants under SD and LD conditions. These results are similar to those for the *OsCOL16* gene in rice.

CO controls flowering by inducing the expression of the downstream gene *FT* [36,50]. In *Arabidopsis*, *CO* promotes flowering by upregulating the expression of *FT* genes under LD conditions and delays flowering by decreasing *FT* gene expression [51]. *CO* homologs, such as the *COL8* and *COL9* genes, repress *FT* expression and repress flowering only under LD conditions [22,52]. In bamboo, *PvCO1* decreases the expression of *FT* to control flowering time [53]. The *OsCOL9* gene delays flowering by repressing the downstream flowering-promoting gene *Ehd1* [54]. In the present experiment, both the *MiCOL16A* and *MiCOL16B* genes repressed flowering by decreasing the expression of *AtSOC1* and *AtFT* under SD and LD conditions (Figure 7). Similarly, the *MiCO* gene also represses flowering by decreasing *AtFT* and *AtSOC1* expression [31]. Together, our findings suggest that the *MiCOL16A* and *MiCOL16B* genes regulate flowering time by affecting the expression levels of *SOC1* and *FT*.

The molecular responses of plants to abiotic stresses are complex and dynamic [55,56], and they involve interactions with many molecular pathways [57]. Similarly, plant responses to these stresses are also complex [58]. *CO* is universally known as a photoperiod-responsive gene [5]. In recent years, some experiments have indicated that *CO* and *CO* homologs have a certain impact on the responses of plants to abiotic stresses. In *Arabidopsis*, the expression of the *AtCOL4* gene is significantly upregulated under high-salt and osmotic stress, and the survival rate of *AtCOL4* transgenic plants is higher than that of *atcol4* and WT plants [59]. The expression level of *GhCOL16*, a *CO* homolog in cotton, was also upregulated 12 h after NaCl or polyethylene glycol (PEG) 6000 treatment [60]. In the present study, the lengths of the roots and survival rates of the *MiCOL16A* and *MiCOL16B* transgenic plants were all greater than those of the WT plants under salt or drought conditions. This result shows that *MiCOL16A* and *MiCOL16B* enhance the tolerance of the transgenic plants to abiotic stress. However, *BnCOL2* increases sensitivity to drought conditions in *Arabidopsis* plants, and *BnCOL2* overexpression results in a survival rate that is lower than that of the WT plants [61]. These results are different from the results of the present experiment and may be caused by the presence of different domains.

To some extent, the transcript levels of stress-related genes also indicate the tolerance of plants to abiotic stresses [62]. For example, stress-responsive gene expression was reduced, resulting in a decrease in the stress tolerance of *BnCOL2* transgenic lines [61]. In our study, all of the *MiCOL16A* and *MiCOL16B* transgenic plants were tolerant to drought and salt stress; the expression levels of *AtNHX1*, *AtRD20* and *AtSOS1* increased under salt treatment; and the expression levels of *AtCOR15A*, *AtRD20* and *AtNHX1* increased under drought treatment. *AtNHX1* and *AtRD20* play vital roles in the response to salt and drought stress [63–65], *AtSOS1* transcript levels substantially increase upon NaCl treatment [66], and the *AtCOR15A* gene is known as a marker of drought stress [67]. In summary, it can be hypothesized that by regulating stress-responsive genes, the *MiCOL16A* and *MiCOL16B* genes positively regulate the salt and drought stress tolerance of *Arabidopsis*.

4. Material and Methods

4.1. Materials

The samples (*M. indica* L. cv. SiJiMi) were collected from an orchard at Guangxi University, Nanning, Guangxi, China. The leaves, buds and stems of nonflowering and flowering branches were collected on 4 January 2019. Leaves were collected on 5 November 2018, 5 December 2018, 4 January 2019, 29 January 2019 and 6 March 2019. Leaves were collected every three hours on three separate days from 2-year-old mango trees grown

under different conditions for diurnal rhythmic expression analysis (LD (16 h light/8 h dark), MD (12 h light/12 h dark) and SD (8 h light/16 h dark)). The plant samples were frozen in liquid nitrogen and kept at -80°C . Wild-type (WT) *Arabidopsis* ecotype Columbia (Col-0) plants were used to study gene function and were grown in the laboratory.

4.2. Identification and Sequence Analysis

Total RNA of SiJiMi mango plants was extracted by using an RNAPrep Pure Kit (for polysaccharide- and polyphenolic-rich plants, DP441) (Tiangen, Beijing, China). cDNA was reverse transcribed with 1 μg of total RNA with PrimeScriptTM Reverse Transcriptase M-MLV (Takara, Dalian, China) and Oligo(dT)18 primers (TTTTTTTTTT TTTTTTTTTTTT). The cetyl-trimethylammonium bromide (CTAB) method was used to isolate genomic DNA from mango leaves [68]. The *MiCOL16* gene was isolated from the transcriptomic data of SiJiMi mango (unpublished data), after which the sequence was verified. The primers designed for cloning included SCOL16Au (5'-GCCTTTGCAA AATGATCACCGG-3'), SCOL16Ad (5'-GCGCCATTTATTCTTGAGG-3'), SCOL16Bu (5'-GTCTTTGCGGTATGAT CACTG-3') and SCOL16Bd (5'-CGGCCATCACCATTTAT TTC-3'). The PCR conditions were as follows: 95°C for 3 min; 38 cycles of 95°C for 30 s, $53^{\circ}\text{C}/52^{\circ}\text{C}$ for 30 s and 72°C for 1 min 30 s; and 72°C for 10 min. The final products were inserted into a pMD18-T vector and sequenced.

The amino acid sequences of *MiCOL16A* and *MiCOL16B* were analyzed with the BLAST search tool (<https://www.ncbi.nlm.nih.gov/BLAST/>, accessed on 20 May 2019). CO homologous sequences were downloaded from the NCBI database (<https://www.ncbi.nlm.nih.gov>, accessed on 25 May 2019). Sequence alignment was subsequently performed using DNAMAN 7 software (Lynnon Corporation, Pointe-Claire, QC, Canada). A neighbor-joining tree based on the CO gene family in *Arabidopsis* and several other tree species was constructed via MEGA 6.06, with 1000 bootstrap replicates.

4.3. qRT-PCR Analysis

First-strand cDNA of each sample was synthesized, and *MiActin1* (qMiACTu, 5'-CCGAGACATGAAGGAGAAGC-3'; qMiACTd, 5'-GTGGTCTCATGGATACCAGCA-3') was used as an internal control gene for data processing [69]. The gene-specific primers used for *MiCOL16A* and *MiCOL16B* were qCOL16Au (5'-TGAATCACCACTG GCAGCTGA-3') and qCOL16Ad (5'-GGGGTTCCTGTTGTCCATGGA-3') as well as qCOL16Bu (5'-ACTTCGGAGACAGCACAGTGA-3') and qCOL16Bd (5'-TTGCATTCGG TGTTCGCCATT-3'). qRT-PCR was performed with an ABI 7500 Real-Time PCR System (Applied Biosystems, Foster City, CA, USA) in conjunction with SYBR Premix Ex Taq II (Takara, Dalian, China). The expression data were normalized according to the $2^{-\Delta\Delta\text{Ct}}$ method [70].

4.4. Subcellular Localization

The *MiCOL16A* and *MiCOL16B* coding DNA sequence (CDS) regions were cloned into a green fluorescent protein (GFP)-encoding gene via the cauliflower mosaic virus (CaMV) 35S promoter. GFP fusions were transferred into *Agrobacterium tumefaciens* EH105, which were then transiently injected into onion inner epidermal cells. Fluorescent cells were observed via laser confocal microscopy. An empty vector with only GFP was used as the control, and 4',6-diamidino-2-phenylindole (DAPI) was used to visualize the location of the nucleus.

4.5. Analysis of Transcriptional Activity of *MiCOL16A* and *MiCOL16B*

To determine the transcriptional activation domains, BD-MiCOL16A, BD-MiCOL16B, BD-MiCOL16A- ΔMR and BD-MiCOL16B- ΔMR constructs were generated, and the full-length CDS and middle region (MR) deletion of *MiCOL16A* and *MiCOL16B* were amplified via PCR and inserted into the pGBKT7 expression vector (Clontech, Dalian, China). An empty pGBKT7 vector was used as a control (BD-vector). These four plasmids and empty pGBKT7 vectors were subsequently transferred into Y2H Gold yeast cells. The seedlings

were subsequently grown on sucrose–dextran (SD) media lacking tryptophan for 3 days. The yeast strains that grew successfully were then transferred onto SD/-Trp, SD/-Trp/X- α -gal and SD/-Trp/X- α -gal/AbA media and grown for another 3 days.

4.6. Vector Construction and Arabidopsis Plant Transformation

The complete CDSs of *MiCOL16A* and *MiCOL16B* were amplified and inserted into a pBI121 vector. The gene-specific primers used were as follows: ZCOL16Au (5'-TCTAGAAT GATCACCGGAAAG-3'; the *Xba* I site is underlined), ZCOL16Ad (5'-CCCCGGTTATTCT TGAGGTAAGG-3'; the *Xma* I site is underlined), ZCOL16Bu (5'-GCGGTTCTAGAATGATC TCTG-3'; the *Xba* I site is underlined) and ZCOL16Bd (5'-CCCCGGTTATTCTTCAGGTAG GG-3'; the *Xma* I site is underlined). The pBI121 vector was subsequently digested by *Xba* I and *Xma* I restriction enzymes. Positive recombinant pBI121-MiCOL16A and pBI121-MiCOL16B plasmids were then transformed into *Agrobacterium tumefaciens* EH105. The primers JCOL16Au (5'-GCCTTTGCAAATGATCACCGG-3'), JCOL16Bu (5'-GTCTTTGC GGTATGATCAC TG-3') and 121GUSd (5'-TTGGGACAACTCCAGTGAAAAG-3') were used to assess the target bacterial colonies. *Arabidopsis* plants were subsequently transformed with the floral-dip method [71]. Transgenic *Arabidopsis* plants growing on half-strength Murashige and Skoog (MS) media supplemented with 50 mg/L kanamycin were identified and then transplanted into square pots filled with a mixture of organic substrate, peat moss and vermiculite (2:2:1), after which they were allowed to grow unabated for 7 days. Seeds of T3-generation homozygous plants were sown at 22 °C under SD conditions (8 h light/16 h darkness) or LD conditions (16 h light/8 h darkness) to measure flowering time, plant height and rosette leaves. Two-week-old WT and transgenic plants were sampled for qRT-PCR analysis. The flowering-related genes *AtSOC1* (No. AY007726; primers F, 5'-CGAGCAAGAAAGACTCAAGTGTTTAAGG-3'; R, 5'-TTCATGAGATCCCCA CTTTTCAGAGAG-3') and *AtFT* (No. AB027504; primers, 5'-CTTGGCAGGCAAACAGTGTATGCAC-3'; R, 5'-GCCACTCTCCCTCTGACAATTG TAGA-3') were used for qRT-PCR analysis.

4.7. Stress Treatments of Transgenic and WT Plants

Seeds of the transgenic lines and WT were sown evenly on the surface of half-strength MS media without antibiotics and stored at 4 °C for 3 days for vernalization.

For root growth assays, WT and *MiCOL16A* and *MiCOL16B* transgenic lines were subjected to stress, and 3 days later, all the plants were transferred to vertically oriented square-shaped containers filled with half-strength MS agar media supplemented with NaCl (0, 100 and 200 mM) or mannitol (0, 300 and 500 mM) [72,73]. The plants were then grown upright in an artificial climate chamber under LD conditions at 22 °C. Seven days later, the length of the primary roots of all lines was measured.

To assess the stress tolerance of transgenic *Arabidopsis*, 7-day-old seedlings were transplanted into square pots. For salt stress, the WT and transgenic lines were treated with 300 mM NaCl solution every 2 days until obvious phenotypic differences occurred, and then the survival rate was determined. For drought treatment, water was withheld from the transgenic lines and WT plants until obvious phenotypic differences occurred. After rewatering for 3 days, the survival rates of the overexpression lines and WT plants were measured.

To investigate the expression patterns of related genes in transgenic *Arabidopsis* plants in response to stress, seeds of the transgenic lines and WT were sown on half-strength MS media supplemented with NaCl or mannitol. Fifteen days later, total RNA was extracted. The specific primers used for the stress-related genes *AtNHX1* (No. AT5G27150; F, 5'-AGCCTTCAGGGAACCAAT-3'; R, 5'-CTCAAAGACGGGTCGC ATG-3') [64], *AtRD20* (No. AT2G33380; F, 5'-ATCGACAACATACACAAAGCCAA-3'; R, 5'-TCCATCAA AGCAACCTCTCACAG-3') [63], *AtSOS1* (No. AT2G01980; F, 5'-AGTGTAAGTTTCGGTG GGATC-3'; R, 5'-CACGCATGTTTACGGGTTTC-3') [74], and *AtCOR15A* (No. AT2G42540; F, 5'-TTCCACAGCGGAGCCAAGCA-3'; R, 5'-AGCGCGTAGATCAACGACTTC-3') [67]

were used to perform qRT-PCR, and *AtActin2* (No. At3g18780; F, 5'-CACTGTGCCAATCTA CGAGGGT-3'; R, 5'-GCTGGAA TGTGCTGAGGGAAG-3') was used as a reference control.

4.8. Statistical Analysis

All experiments were repeated at least three times. The standard deviations (SDs) are represented by error bars in the figures. All statistical analyses were performed by SPSS 17.0, and significance was tested at the $p < 0.05$ (* in the figures) and $p < 0.01$ (** or Lowercase letters in the figures) levels. Bar charts were generated with GraphPad Prism 7 software.

5. Conclusions

In this study, we isolated the *MiCOL16A* and *MiCOL16B* genes from SiJiMi mango. Both the *MiCOL16A* and *MiCOL16B* proteins localize to the nucleus and have transcriptional activity through their MR domain. Overexpression of *MiCOL16A* and *MiCOL16B* repressed flowering in *Arabidopsis* under SD and LD conditions and improved tolerance to drought and salt stress conditions. Overall, our results clearly demonstrated that the *MiCOL16A* and *MiCOL16B* genes play key roles in mango flowering and abiotic stress responses.

Supplementary Materials: The following supporting information can be downloaded at: <https://www.mdpi.com/article/10.3390/ijms23063075/s1>.

Author Contributions: X.H. and C.L. conceived and designed the experiments; Y.L., Y.G. and R.L. performed this experiment; C.L., H.Y. and X.M. provided technical assistance; S.C. and X.Y. collected and analyzed the data; Y.L. wrote the manuscript; C.L. and X.H. revised the manuscript. All authors have read and agreed to the published version of the manuscript.

Funding: This research was supported by the National Natural Science Foundation of China (31860541), State Key Laboratory for Conservation and Utilization of Subtropical Agro-bioresources (SKLCUSA-a201906, SKLCUSA-c201901), Innovation Team of Guangxi Mango Industry Project (nycytxgxcxd-2021-06-02), the sixth special action of “strengthening agriculture and enriching people” by science and technology Vanguard (Guangxi Agricultural Science and technology League 202204).

Institutional Review Board statement: Not applicable.

Informed Consent Statement: Not applicable.

Conflicts of Interest: The authors declare no conflict of interest.

References

- Okamoto, J.K.; Szeto, W.; Lotys-Prass, C.; Jofuku, K.D. Photo and hormonal control of meristem identity in the *Arabidopsis* flower mutants *apetala2* and *apetala1*. *Plant Cell* **1997**, *9*, 37–47. [PubMed]
- Wu, G.; Park, M.Y.; Conway, S.R.; Wang, J.W.; Weigel, D.; Poethig, R.S. The sequential action of miR156 and miR172 regulates developmental timing in *Arabidopsis*. *Cell* **2009**, *138*, 750–759. [CrossRef] [PubMed]
- Blazquez, M.A.; Green, R.; Nilsson, O.; Sussman, M.R.; Weigel, D. Gibberellins promote flowering of *Arabidopsis* by activating the *LEAFY* promoter. *Plant Cell* **1998**, *10*, 791–800. [CrossRef]
- Huang, G.W.; Ma, J.H.; Han, Y.Z.; Chen, X.J.; Fu, Y.F. Cloning and expression analysis of the soybean *CO-like* gene *GmCOL9*. *Plant Mol. Biol. Rep.* **2010**, *29*, 352–359. [CrossRef]
- Komeda, Y. Genetic regulation of time to flower in *Arabidopsis thaliana*. *Annu. Rev. Plant Biol.* **2004**, *55*, 521–553. [CrossRef]
- Putterill, J.; Robson, F.; Lee, K.; Simon, R.; Coupland, G. The *CONSTANS* gene of *Arabidopsis* promotes flowering and encodes a protein showing similarities to zinc finger transcription factors. *Cell* **1995**, *80*, 847–857. [CrossRef]
- Griffiths, S.; Dunford, R.P.; Coupland, G.; Laurie, D.A. The evolution of *CONSTANS-like* gene families in barley, rice, and *Arabidopsis*. *Plant Physiol.* **2003**, *131*, 1855–1867. [CrossRef]
- Yano, M.; Katayose, Y.; Ashikari, M.; Yamanouchi, U.; Monna, L.; Fuse, T.; Baba, T.; Yamamoto, K.; Umehara, Y.; Nagamura, Y.; et al. *Hd1*, a major photoperiod sensitivity quantitative trait locus in rice, is closely related to the *Arabidopsis* flowering time gene *CONSTANS*. *Plant Cell* **2000**, *12*, 2473–2484. [CrossRef]
- Serrano, G.; Herrera-Palau, R.; Romero, J.M.; Serrano, A.; Coupland, G.; Valverde, F. *Chlamydomonas* *CONSTANS* and the evolution of plant photoperiodic signaling. *Curr. Biol.* **2009**, *19*, 359–368. [CrossRef]
- Imaizumi, T.; Schultz, T.F.; Harmon, F.G.; Ho, L.A.; Kay, S.A. FKF1 F-box protein mediates cyclic degradation of a repressor of *CONSTANS* in *Arabidopsis*. *Science* **2005**, *309*, 293–297. [CrossRef]

11. Sawa, M.; Nusinow, D.A.; Kay, S.A.; Imaizumi, T. *FKF1* and *GIGANTEA* complex formation is required for day-length measurement in *Arabidopsis*. *Science* **2007**, *318*, 261–265. [[CrossRef](#)] [[PubMed](#)]
12. Imaizumi, T.; Kay, S.A. Photoperiodic control of flowering: Not only by coincidence. *Trends Plant Sci.* **2006**, *11*, 550–558. [[CrossRef](#)] [[PubMed](#)]
13. Wigge, P.A.; Kim, M.C.; Jaeger, K.E.; Busch, W.; Schmid, M.; Lohmann, J.U.; Weigel, D. Integration of spatial and temporal information during floral induction in *Arabidopsis*. *Science* **2005**, *309*, 1056–1059. [[CrossRef](#)] [[PubMed](#)]
14. Shogo, I.; Young, H.S.; Anna, R.J.; Ryan, J.M.; Ghislain, B.; Richard, G.O.; Takato, I. *FLOWERING BHLH* transcriptional activators control expression of the photoperiodic flowering regulator *CONSTANS* in *Arabidopsis*. *Proc. Natl. Acad. Sci. USA* **2012**, *109*, 3582–3587.
15. Sun, J.J.; Lu, J.; Bai, M.J.; Chen, Y.Q.; Wang, W.N.; Fan, C.G.; Liu, J.Y.; Ning, G.G.; Wang, C.Q. Phytochrome-interacting factors interact with transcription factor *CONSTANS* to suppress flowering in rose. *Plant Physiol.* **2021**, *186*, 1186–1201. [[CrossRef](#)]
16. Ana, L.; Federico, V.; Manuel, P.; Jose, A.J. The *Arabidopsis* E3 ubiquitin ligase *HOS1* negatively regulates *CONSTANS* abundance in the photoperiodic control of flowering. *Plant Cell* **2012**, *24*, 982–999.
17. Liu, L.J.; Zhang, Y.C.; Li, Q.H.; Sang, Y.; Mao, J.; Lian, H.L.; Wang, L.; Yang, H.Q. COP1-Mediated ubiquitination of *CONSTANS* is implicated in cryptochrome regulation of flowering in *Arabidopsis*. *Plant Cell* **2008**, *20*, 292–306. [[CrossRef](#)]
18. Yang, N.; Cong, Q.; Cheng, L.J. *BBX* transcriptional factors family in plants—a review. *Chin. J. Biotechnol.* **2019**, *36*, 666–677.
19. Ledger, S.; Strayer, C.; Ashton, F.; Kay, S.A.; Putterill, J. Analysis of the function of two circadian-regulated *CONSTANS-LIKE* genes. *Plant J.* **2001**, *26*, 15–22. [[CrossRef](#)]
20. Graeff, M.; Straub, D.; Eguen, T.; Dolde, U.; Rodrigues, V.; Brandt, R.; Wenkel, S. Microprotein-mediated recruitment of *CONSTANS* into a topless trimeric complex represses flowering in *Arabidopsis*. *PLoS Genet.* **2016**, *12*, e1005959. [[CrossRef](#)]
21. Wang, H.G.; Zhang, Z.L.; Li, H.Y.; Zhao, X.Y.; Liu, X.M.; Ortiz, M.; Lin, C.T.; Liu, B. *CONSTANS-LIKE 7* regulates branching and shade avoidance response in *Arabidopsis*. *J. Exp. Bot.* **2013**, *64*, 1017–1024. [[CrossRef](#)] [[PubMed](#)]
22. Takase, T.; Kakikubo, Y.; Nakasone, A.; Nishiyama, Y.; Yasuhara, M.; Yoko, T.; Kiyosue, T. Characterization and transgenic study of *CONSTANS-LIKE8 (COL8)* gene in *Arabidopsis thaliana*: Expression of 35S:COL8 delays flowering under long-day conditions. *Plant Biotechnol.* **2011**, *28*, 439–446. [[CrossRef](#)]
23. Tsuji, H.; Taoka, K.; Shimamoto, K. Regulation of flowering in rice: Two florigen genes, a complex gene network, and natural variation. *Curr. Opin. Plant Biol.* **2011**, *14*, 45–52. [[CrossRef](#)]
24. Wu, W.X.; Zheng, X.M.; Chen, D.B.; Zhang, Y.X.; Ma, W.W.; Zhang, H.; Sun, L.P.; Yang, Z.F.; Zhao, C.D.; Zhan, X.D.; et al. *OsCOL16*, encoding a *CONSTANS-like* protein, represses flowering by upregulating *Ghd7* expression in rice. *Plant Sci.* **2017**, *260*, 60–69. [[CrossRef](#)] [[PubMed](#)]
25. Gonzalez-Schain, N.D.; Diaz-Mendoza, M.; Zurczak, M.; Suárez-López, P. Potato *CONSTANS* is involved in photoperiodic tuberization in a graft-transmissible manner. *Plant J.* **2012**, *70*, 678–690. [[CrossRef](#)] [[PubMed](#)]
26. Jeong, D.H.; Sung, S.K.; An, G. Molecular cloning and characterization of *CONSTANS-like* cDNA clones of the Fuji apple. *J Plant Biol.* **1999**, *42*, 23–31. [[CrossRef](#)]
27. Luo, C.; Yu, H.X.; Fan, Y.; Zhang, X.J.; He, X.H. Research advance on the flowering mechanism of mango. *Acta Hortic.* **2019**, *1244*, 2. [[CrossRef](#)]
28. Fan, Z.Y.; He, X.H.; Fan, Y.; Yu, H.X.; Wang, Y.H.; Xie, X.J.; Liu, Y.; Mo, X.; Wang, J.Y.; Luo, C. Isolation and functional characterization of three *MiFTs* genes from mango. *Plant Physiol. Biochem.* **2020**, *155*, 169–176. [[CrossRef](#)]
29. Wei, J.Y.; Liu, D.B.; Liu, G.Y.; Tang, J.; Chen, Y.Y. Molecular cloning, characterization, and expression of *MiSOC1*: A homolog of the flowering gene *SUPPRESSOR OF CONSTANS1* from mango (*Mangifera indica* L.). *Front. Plant Sci.* **2016**, *7*, 1758. [[CrossRef](#)]
30. Yu, H.X.; Luo, C.; Fan, Y.; Zhang, X.J.; Huang, F.; Li, M.; He, X.H. Isolation and characterization of two *APETALA1-Like* genes from mango (*Mangifera indica* L.). *Sci. Hortic.* **2020**, *259*, 108814. [[CrossRef](#)]
31. Liu, Y.; Luo, C.; Zhang, X.J.; Lu, X.X.; Yu, H.X.; Xie, X.J.; Fan, Z.Y.; Mo, X.; He, X.H. Overexpression of the mango *MiCO* gene delayed flowering time in transgenic *Arabidopsis*. *Plant Cell Tissue Organ Cult.* **2020**, *143*, 219–228. [[CrossRef](#)]
32. Tan, J.J.; Jin, M.N.; Wang, J.C.; Wu, F.Q.; Sheng, P.K.; Cheng, Z.J.; Wang, J.L.; Zheng, X.M.; Chen, L.P.; Wang, M.; et al. *OsCOL10*, a *CONSTANS-Like* gene, functions as a flowering time repressor downstream of *Ghd7* in rice. *Plant Cell Physiol.* **2016**, *57*, 798–812. [[CrossRef](#)] [[PubMed](#)]
33. Wu, W.X.; Zhang, Y.X.; Zhang, M.; Zhan, X.D.; Shen, X.H.; Yu, P.; Chen, D.B.; Liu, Q.E.; Sinumporn, S.; Hussain, K.; et al. The rice *CONSTANS-like* protein *OsCOL15* suppresses flowering by promoting *Ghd7* and repressing *RID1*. *Biochem. Biophys. Res. Commun.* **2018**, *495*, 1349–1355. [[CrossRef](#)]
34. Valverde, F. *CONSTANS* and the evolutionary origin of photoperiodic timing of flowering. *J. Exp. Bot.* **2011**, *62*, 2453–2463. [[CrossRef](#)] [[PubMed](#)]
35. Yan, J.; Mao, D.; Liu, X.M.; Wang, L.L.; Xu, F. Isolation and functional characterization of a circadian-regulated *CONSTANS* homolog (*GbCO*) from *Ginkgo biloba*. *Plant Cell Rep.* **2017**, *36*, 1387–1399. [[CrossRef](#)]
36. Samach, A.; Onouchi, H.; Gold, S.E.; Ditta, G.S.; Schwarz-Sommer, Z.; Yanofsky, M.F.; Coupland, G. Distinct roles of *CONSTANS* target genes in reproductive development of *Arabidopsis*. *Science* **2000**, *288*, 1613–1616. [[CrossRef](#)]
37. Sawa, M.; Kay, S.A. *GIGANTEA* directly activates *FLOWERING LOCUS T* in *Arabidopsis thaliana*. *Proc. Natl. Acad. Sci. USA* **2011**, *108*, 11698–11703. [[CrossRef](#)]

38. Turck, F.; Fornara, F.; Coupland, G. Regulation and identity of florigen: *FLOWERING LOCUS T* moves center stage. *Annu. Rev. Plant Biol.* **2008**, *59*, 573–594. [[CrossRef](#)]
39. Bohlenius, H.; Huang, T.; Charbonnelcampaa, L.; Brunner, A.M.; Jansson, S.; Strauss, S.H.; Nilsson, O. *CO/FT* regulatory module controls timing of flowering and seasonal growth cessation in trees. *Science* **2006**, *312*, 1040–1043. [[CrossRef](#)]
40. Wang, L.L.; Yan, J.P.; Meng, X.X.; Ye, J.B.; Zhang, W.W.; Xu, F. Cloning and expression analysis of *CONSTANS-like 16* (*GbCOL16*) gene from *Ginkgo biloba*. *BMC Biotechnol.* **2017**, *16*, 92–99. [[CrossRef](#)]
41. Chia, T.Y.P.; Muller, A.; Jung, C.; Mutasa-Gottgens, E.S. Sugar beet contains a large *CONSTANS-like* gene family including a *CO* homologue that is independent of the early-bolting (*B*) gene locus. *J. Exp. Bot.* **2008**, *59*, 2735–2748. [[CrossRef](#)] [[PubMed](#)]
42. Akemi, O.; Chihiro, O.Y.; Sanae, K. Overexpression of *CONSTANS-like 16* enhances chlorophyll accumulation in petunia corollas. *Plant Sci.* **2019**, *280*, 90–96.
43. Wang, L.; Xue, J.; Dai, W.; Tang, Y.; Gong, P.; Wang, Y.; Zhang, C. Genome-wide identification, phylogenetic analysis, and expression profiling of *CONSTANS-like* (*COL*) genes in *vitis vinifera*. *J. Plant Growth Regul.* **2019**, *38*, 631–643. [[CrossRef](#)]
44. Suarez-Lopez, P.; Wheatley, K.; Robson, F. *CONSTANS* mediates between the circadian clock and the control of flowering in *Arabidopsis*. *Nature* **2001**, *410*, 1116–1120. [[CrossRef](#)] [[PubMed](#)]
45. Zhang, J.X.; Zhao, X.L.; Tian, R.X.; Zeng, S.J.; Wu, K.L.; Silva, J.A.; Duan, J. Molecular cloning and functional analysis of three *CONSTANS-Like* genes from Chinese Cymbidium. *J. Plant Growth Regul.* **2019**, *39*, 1061–1074. [[CrossRef](#)]
46. Zhang, Z.; Ji, R.; Li, H.; Tao, Z.; Liu, J.; Lin, C.; Liu, B. *CONSTANS-LIKE 7* (*COL7*) is involved in phytochrome B (phyB)-mediated light-quality regulation of auxin homeostasis. *Mol. Plant* **2014**, *7*, 1674–2052. [[CrossRef](#)] [[PubMed](#)]
47. Song, Y.H.; Shim, J.S.; Kinmonth-Schultz, H.A.; Imaizumi, T. Photoperiodic flowering: Time measurement mechanisms in leaves. *Annu. Rev. Plant Biol.* **2015**, *66*, 441–464. [[CrossRef](#)] [[PubMed](#)]
48. Steinbach, Y. The *Arabidopsis thaliana* *CONSTANS-LIKE 4* (*COL4*) a modulator of flowering time. *Front. Plant Sci.* **2019**, *10*, 651. [[CrossRef](#)]
49. Kim, S.K.; Yun, C.H.; Lee, J.H.; Jang, Y.H.; Park, H.Y.; Kim, J.K. *OsCO3*, a *CONSTANS-LIKE* gene, controls flowering by negatively regulating the expression of *FT-like* genes under SD conditions in rice. *Planta* **2008**, *228*, 355–365. [[CrossRef](#)]
50. Kardailsky, I.; Shukla, V.K.; Ahn, J.H.; Dagenais, N.; Christensen, S.K.; Nguyen, J.T.; Chory, J.; Harrison, M.J.; Weigel, D. Activation tagging of the floral inducer *FT*. *Science* **1999**, *286*, 1962–1965. [[CrossRef](#)]
51. Luccioni, L.; Krzymuski, M.; Sanchez-Lamas, M.; Karayekov, E.; Cerdan, P.D.; Casal, J.J. *CONSTANS* delays *Arabidopsis* flowering under short days. *Plant J.* **2019**, *97*, 923–932. [[CrossRef](#)] [[PubMed](#)]
52. Cheng, X.F.; Wang, Z.Y. Overexpression of *COL9*, a *CONSTANS-LIKE* gene, delays flowering by reducing expression of *CO* and *FT* in *Arabidopsis thaliana*. *Plant J.* **2005**, *43*, 758–768. [[CrossRef](#)] [[PubMed](#)]
53. Xiao, G.H.; Li, B.J.; Chen, H.J.; Wang, Z.Y.; Mao, B.Z.; Gui, R.Y.; Guo, X.Q. Overexpression of *PvCO1*, a bamboo *CONSTANS-LIKE* gene, delays flowering by reducing expression of the *FT* gene in transgenic *Arabidopsis*. *BMC Plant Biol.* **2018**, *18*, 232. [[CrossRef](#)]
54. Liu, H.; Gu, F.W.; Dong, S.Y.; Liu, W.; Wang, H.; Chen, Z.Q.; Wang, J.F. *CONSTANS-like 9* (*COL9*) delays the flowering time in *Oryza sativa* by repressing the *Ehd1* pathway. *Biochem. Biophys. Res. Commun.* **2016**, *479*, 173–178. [[CrossRef](#)]
55. Cramer, G.R. Abiotic stress & plant responses from the whole vine to the genes. *Aust. J. Grape Wine Res.* **2010**, *16*, 86–93.
56. Skirycz, A.; Inze, D. More from less: Plant growth under limited water. *Curr. Opin. Biotechnol.* **2010**, *21*, 197–203. [[CrossRef](#)] [[PubMed](#)]
57. Takahashi, S.; Seki, M.; Ishida, J.; Satou, M.; Sakurai, T.; Narusaka, M.; Kamiya, A.; Nakajima, M.; Enju, A.; Akiyama, K.; et al. Monitoring the expression profiles of genes induced by hyperosmotic, high salinity, and oxidative stress and abscisic acid treatment in *Arabidopsis* cell culture using a full-length cDNA microarray. *Plant Mol. Biol.* **2004**, *56*, 29–55. [[CrossRef](#)] [[PubMed](#)]
58. Cramer, G.R.; Urano, K.; Delrot, S.; Pezzotti, M.; Shinozaki, K. Effects of abiotic stress on plants: A systems biology perspective. *BMC Plant Biol.* **2011**, *11*, 163. [[CrossRef](#)]
59. Min, J.H.; Chung, J.S.; Lee, K.H.; Kim, C.S. The *CONSTANS-like 4* transcription factor, *AtCOL4*, positively regulates abiotic stress tolerance through an abscisic acid-dependent manner in *Arabidopsis*. *J. Integr. Plant Biol.* **2015**, *57*, 313–324. [[CrossRef](#)]
60. Qin, W.Q.; Yu, Y.; Jin, Y.Y.; Wang, X.D.; Liu, J.; Xi, J.P.; Li, Z.; Li, H.Q.; Zhao, G.; Hu, W.; et al. Genome-wide analysis elucidates the role of *CONSTANS-like* genes in stress responses of cotton. *Int. J. Mol. Sci.* **2018**, *19*, 2658. [[CrossRef](#)]
61. Liu, L.D.; Ding, Q.Y.; Liu, J.; Yang, C.L.; Chen, Y.; Zhang, S.F.; Zhu, J.C.; Wang, D.J. *Brassica napus* *COL* transcription factor *BnCOL2* negatively affects the tolerance of transgenic *Arabidopsis* to drought stress *Environ. Exp. Bot.* **2020**, *178*, 104171. [[CrossRef](#)]
62. Xiong, L.; Schumaker, K.S.; Zhu, J.K. Cell signaling during cold, drought, and salt stress. *Plant Cell* **2002**, *14*, S165–S183. [[CrossRef](#)] [[PubMed](#)]
63. Aubert, Y.; Vile, D.; Pervent, M.; Aldon, D.; Ranty, B.; Simonneau, T.; Vavasseur, A.; Galau, J.P. *RD20*, a stress-inducible caleosin, participates in stomatal control, transpiration and drought tolerance in *Arabidopsis thaliana*. *Plant Cell Physiol.* **2010**, *51*, 1975–1987. [[CrossRef](#)] [[PubMed](#)]
64. Asif, M.A.; Zafar, Y.; Iqbal, J.; Iqbal, M.M.; Rashid, U.; Ali, G.M.; Arif, A.; Nazir, F. Enhanced expression of *AtNHX1*, in transgenic groundnut (*Arachis hypogaea* L.) improves salt and drought tolerance. *Mol. Biotechnol.* **2011**, *49*, 250–256. [[CrossRef](#)] [[PubMed](#)]
65. Wright, J. *RD20/CLO3*, a Stress-Induced Calcium-Binding Protein, Acts as a Negative Regulator of *GPA1* in *Arabidopsis* through *GAP* Activity. Ph.D. Thesis, Concordia University, Montreal, QC, Canada, 2014.
66. Shi, H.; Lee, B.H.; Wu, S.J.; Zhu, J.K. Overexpression of a plasma membrane *Na⁺/H⁺* antiporter gene improves salt tolerance in *Arabidopsis thaliana*. *Nat. Biotechnol.* **2003**, *21*, 81–85. [[CrossRef](#)]

67. Meng, L.S.; Wang, Z.B.; Yao, S.Q.; Liu, A. The *ARF2-ANT-COR15A* gene cascade regulates ABA-signaling-mediated resistance of large seeds to drought in *Arabidopsis*. *J. Cell Sci.* **2015**, *128*, 3922–3932. [[PubMed](#)]
68. Yu, H.X.; Luo, C.; Xu, C.; He, X.H. A simple and efficient method for high quality DNA extraction from transgenic *Arabidopsis* and Tobacco. *Mol. Plant Breed.* **2016**, *14*, 1436–1440.
69. Luo, C.; He, X.H.; Chen, H.; Hu, Y.; Ou, S.J. Molecular cloning and expression analysis of four action genes (*MiACT*) from mango. *Biol. Plantarum.* **2013**, *57*, 238–244. [[CrossRef](#)]
70. Libak, K.J.; Schmittgen, T.D. Analysis of relative gene expression data using real-time quantitative PCR and the $2^{-\Delta\Delta C_t}$ method. *Methods* **2001**, *25*, 402–408.
71. Clough, S.J.; Bent, A.F. Floral dip: A simplified method for *Agrobacterium*-mediated transformation of *Arabidopsis thaliana*. *Plant J.* **1998**, *16*, 735–743. [[CrossRef](#)]
72. Lu, X.; Zhang, X.F.; Duan, H.; Lian, C.L.; Liu, C.; Yin, W.L.; Xia, X.L. Three stress-responsive *NAC* transcription factors from *Populus euphratica* differentially regulate salt and drought tolerance in transgenic plants. *Physiol. Plantarum.* **2017**, *162*, 73–97. [[CrossRef](#)]
73. Pla, M.; Vilardell, J.; Guiltinan, M.J.; Marcotte, W.R.; Niogret, M.F.; Quatrano, R.S.; Pages, M. The cis-regulatory element CCACGTGG is involved in ABA and water-stress responses of the maize gene *rab28*. *Plant Mol. Biol.* **1993**, *21*, 259–266. [[CrossRef](#)]
74. Li, S.X.; Liu, J.L.; An, Y.R.; Cao, Y.M.; Liu, Y.S.; Zhang, J.; Geng, J.C.; Hu, T.M.; Yang, P.Z. *MsPIP2;2*, a novel aquaporin gene from *Medicago sativa*, confers salt tolerance in transgenic *Arabidopsis*. *Environ. Exp. Bot.* **2019**, *165*, 39–52. [[CrossRef](#)]